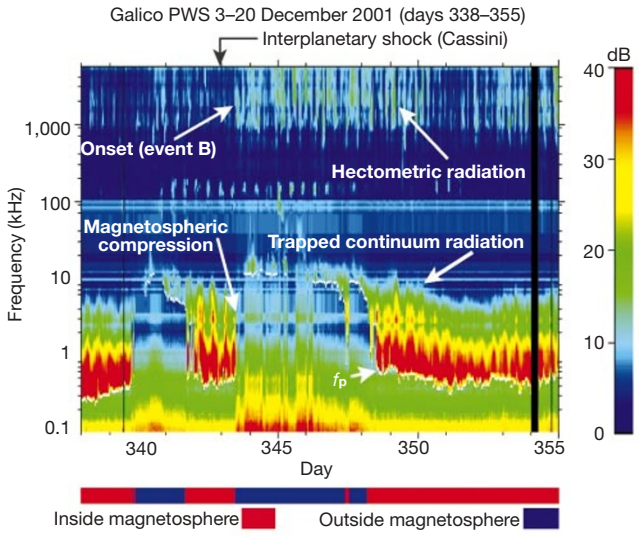

Figure 4 A frequency–time spectrogram from the Galileo PWS showing the radio emission intensities detected by Galileo during event B. The time of the interplanetary shock responsible for this event, as detected by Cassini (at 23:12 UT on day 342), is indicated by the arrow at the top of the spectrogram. The arrival of this shock at Jupiter is believed to be indicated by the disappearance of the trapped continuum radiation at 12:10 UT on day 343, which indicates a sudden compression of the magnetosphere. The white line at the bottom edge of the trapped continuum radiation is the electron plasma frequency, which is proportional to the square root of the electron density. The colour bar at the bottom of the spectrogram indicates when the spacecraft is inside or outside the magnetosphere, on the basis of the presence or absence of the continuum radiation. As can be seen, the onset of the hectometric radiation occurs essentially coincident with the sudden magnetospheric compression on day 343.

altitudes (1 to 3 planetary radii)[14,21] by the cyclotron maser mechanism[10,22]. No *in situ* measurements are available in the high-latitude auroral regions of the jovian magnetosphere, so we use our knowledge of terrestrial auroral processes to help us to understand the processes that are occurring in the jovian magnetosphere. For example, when an interplanetary shock interacts with Earth's magnetosphere, it is known that the magnetosphere becomes strongly compressed. The resulting compression leads to a large-scale reconfiguration of the magnetic field and associated acceleration and energization of plasma within the magnetosphere. The stresses associated with the compression lead to large field-aligned currents and electric fields, particularly along the high-latitude magnetic field lines, where the electrons that carry the field-aligned currents strike the atmosphere and produce the aurora. Very detailed measurements now exist from Earth-orbiting satellites that show how the electrons involved in this process produce the terrestrial auroral kilometric radiation via the cyclotron maser mechanism[23,24]. We infer that similar processes are responsible for the jovian hectometric radiation. At Earth the auroral kilometric radiation is known to be generated along magnetic field lines that terminate in bright spots in the aurora[25]. Because the jovian aurora is also known to have considerable fine structure[26], we can also infer that the discrete arc-like structure evident in the hectometric radiation (see Fig. 1) is most probably associated with the fine structure in the jovian aurora. □

Received 3 August; accepted 1 November 2001.

1. Burke, B. F. & Franklin, K. L. Observations of a variable radio source associated with the planet Jupiter. *J. Geophys. Res.* **60,** 213–217 (1955).
2. Drake, F. D. & Hvatum, S. Non-thermal microwave radiation from Jupiter. *Astron. J.* **64,** 329–330 (1959).
3. Warwick, J. W. Radiophysics of Jupiter. *Space Sci. Rev.* **6,** 841–891 (1967).
4. Broadfoot, A. L. *et al.* Extreme ultraviolet observations from Voyager 1 encounter with Jupiter. *Science* **204,** 979–982 (1979).
5. Chamberlain, J. W. *Physics of the Aurora and Airglow* (Academic, New York, 1961).
6. Carr, T. D., Desch, M. D. & Alexander, J. K. in *Physics of the Jovian Magnetosphere* (ed. Dessler, A. J.) 226–284 (Cambridge Univ. Press, Cambridge, 1983).
7. Clarke, J. T., Moos, H. W., Atreya, S. K. & Lane, A. L. Observations from Earth orbit and variability of the polar aurora on Jupiter. *Astrophys. J.* **241,** L179–L1182 (1980).
8. Gurnett, D. A. *et al.* The Cassini radio and plasma wave investigation. *Space Sci. Rev.* (in the press).
9. Warwick, J. W. *et al.* Voyager 1 planetary radio astronomy observations near Jupiter. *Science* **204,** 995–998 (1979).
10. Wu, C. S. & Lee, L. C. A theory of terrestrial kilometric radiation. *Astrophys. J.* **213,** 621–626 (1979).
11. Bigg, E. K. Influence of the satellite Io on Jupiter's decametric radiation. *Nature* **203,** 1008–1010 (1964).
12. Goldreich, P. & Lynden-Bell, D. Io, a unipolar inductor. *Astrophys. J.* **156,** 59–78 (1969).
13. Queinnec, J. & Zarka, P. Io-controlled decametric arcs and Io–Jupiter interaction. *J. Geophys. Res.* **103,** 26649–26666 (1998).
14. Ladreiter, H. P., Zarka, P. & Lecacheux, A. Direction finding study of Jovian hectometric and broadband kilometric radio emissions: Evidence for their auroral origin. *Planet. Space Sci.* **42,** 919–931 (1994).
15. Zarka, P. & Genova, F. Low-frequency Jovian emission and solar wind magnetic sector structure. *Nature* **306,** 767–768 (1983).
16. Desch, M. D. & Barrow, C. H. Direct evidence for solar wind control of Jupiter's hectometer-wavelength radio emission. *J. Geophys. Res.* **89,** 6819–6823 (1984).
17. Gurnett, D. A. *et al.* The Galileo plasma wave investigation. *Space Sci. Rev.* **60,** 341–355 (1992).
18. Scarf, F. L., Gurnett, D. A. & Kurth, W. S. Jupiter plasma wave observations: an initial Voyager 1 overview. *Science* **204,** 991–995 (1979).
19. Gurnett, D. A. The Earth as a radio source: terrestrial kilometric radiation. *J. Geophys. Res.* **79,** 4227–4238 (1974).
20. Voots, G. R., Gurnett, D. A. & Akasofu, S.-Y. Auroral kilometric radiation as an indicator of auroral magnetic disturbances. *J. Geophys. Res.* **82,** 2259–2266 (1977).
21. Gallagher, D. L. & Gurnett, D. A. Auroral kilometric radiation: time-averaged source location. *J. Geophys. Res.* **84,** 6501–6509 (1979).
22. Zarka, P. Auroral radio emissions at the outer planets: observations and theories. *J. Geophys. Res.* **103,** 20159–20194 (1998).
23. Louarn, P. *et al.* Trapped electrons as a free energy source for the auroral kilometric radiation. *J. Geophys. Res.* **95,** 5983–5995 (1990).
24. Ergun, R. E. *et al.* Electron-cyclotron maser driven by charge particle acceleration from magnetic field-alligned electric fields. *Astrophys. J.* **538,** 456–466 (2000).
25. Huff, R. L. Mapping of auroral kilometric radiation sources to the aurora. *J. Geophys. Res.* **93,** 11445–11454 (1988).
26. Clarke, J. T. *et al.* Hubble Space Telescope imaging of Jupiter's UV aurora during the Galileo orbiter mission. *J. Geophys. Res.* **103,** 20217–20236 (1998).
27. Dougherty, M. K. *et al.* The Cassini magnetic field investigation. *Space Sci. Rev.* (submitted).
28. Young, D. T. *et al.* Cassini plasma spectrometer investigation. *Space Sci. Rev.* (submitted).
29. Esposito, L. W. *et al.* The Cassini ultraviolet imaging spectrograph investigation. *Space Sci. Rev.* (in the press).

Acknowledgements

The research at the University of Iowa, the University of Michigan, and the University of Colorado was supported by NASA through the Jet Propulsion Laboratory.

Correspondence and requests for materials should be addressed to D.A.G. (e-mail: donald-gurnett@iowa.edu).

Ultra-relativistic electrons in Jupiter's radiation belts

S. J. Bolton*, M. Janssen*, R. Thorne†, S. Levin*, M. Klein*, S. Gulkis*, T. Bastian‡, R. Sault§, C. Elachi*, M. Hofstadter*, A. Bunker*, G. Dulk‖, E. Gudim*, G. Hamilton*, W. T. K. Johnson*, Y. Leblanc‖, O. Liepack*, R. McLeod¶, J. Roller¶, L. Roth* & R. West*

** Jet Propulsion Laboratory/Caltech, Pasadena, California 91109, USA*
† University of California, Department of Atmospheric Sciences, Los Angeles, California 90024, USA
‡ National Radio Astronomy Observatory, Charlottesville, Virginia 24944, USA
§ Australia Telescope National Facility, Epping, New South Wales 1710, Australia
‖ Observatory of Paris, Department of Space Research, F-92195 Meudon, France
¶ Lewis Center for Educational Research, Apple Valley, California 92307, USA

Ground-based observations have shown that Jupiter is a two-component source of microwave radio emission[1]: thermal atmospheric emission and synchrotron emission[2] from energetic electrons spiralling in Jupiter's magnetic field. Later *in situ* measurements[3,4] confirmed the existence of Jupiter's high-energy electron-radiation belts, with evidence for electrons at

energies up to 20 MeV. Although most radiation belt models predict electrons at higher energies[5,6], adiabatic diffusion theory can account only for energies up to around 20 MeV. Unambiguous evidence for more energetic electrons is lacking. Here we report observations of 13.8 GHz synchrotron emission that confirm the presence of electrons with energies up to 50 MeV; the data were collected during the Cassini fly-by of Jupiter. These energetic electrons may be repeatedly accelerated through an interaction with plasma waves, which can transfer energy into the electrons. Preliminary comparison of our data with model results suggests that electrons with energies of less than 20 MeV are more numerous than previously believed.

On 2–3 January 2001, *en route* to Saturn, measurements of Jupiter's synchrotron emission were successfully carried out using the radiometer subsystem of the Cassini radar instrument[7] operating at 2.2 cm (13.8 GHz). Synchrotron radiation is the relativistic counterpart to cyclotron radiation (the emission originates from the gyration motion of trapped electrons). Relativistic effects cause the continuum emission to be radiated in a narrow beam focused in the direction of the electron's motion. The spectrum of synchrotron radiation is characterized by a well defined peak frequency that depends on both electron energy and magnetic field magnitude. Observations at different frequencies (assuming equivalent magnetic field magnitude) relate to emission from electrons at different energies; however, owing to confusion with thermal emission, ground-based telescopes have difficulty observing synchrotron emission at frequencies higher than ~5 GHz. Cassini's proximity to Jupiter and the excellent sensitivity of the radar instrument offered an opportunity to map and accurately measure Jupiter's synchrotron emission at a higher frequency than is possible with ground-based telescopes. The motivation was to constrain the high end of the energy spectrum of the electrons trapped in Jupiter's radiation belts. Simultaneous ground-based observations at a wide range of frequencies were carried out to obtain data corresponding to emission from ~5 MeV to >50 MeV electrons. Interferometric maps were obtained with the Very Large Array (VLA) operating at 20 cm (1,400 MHz) and 90 cm (333 MHz). Single-dish total flux density measurements were obtained with the Deep Space Network

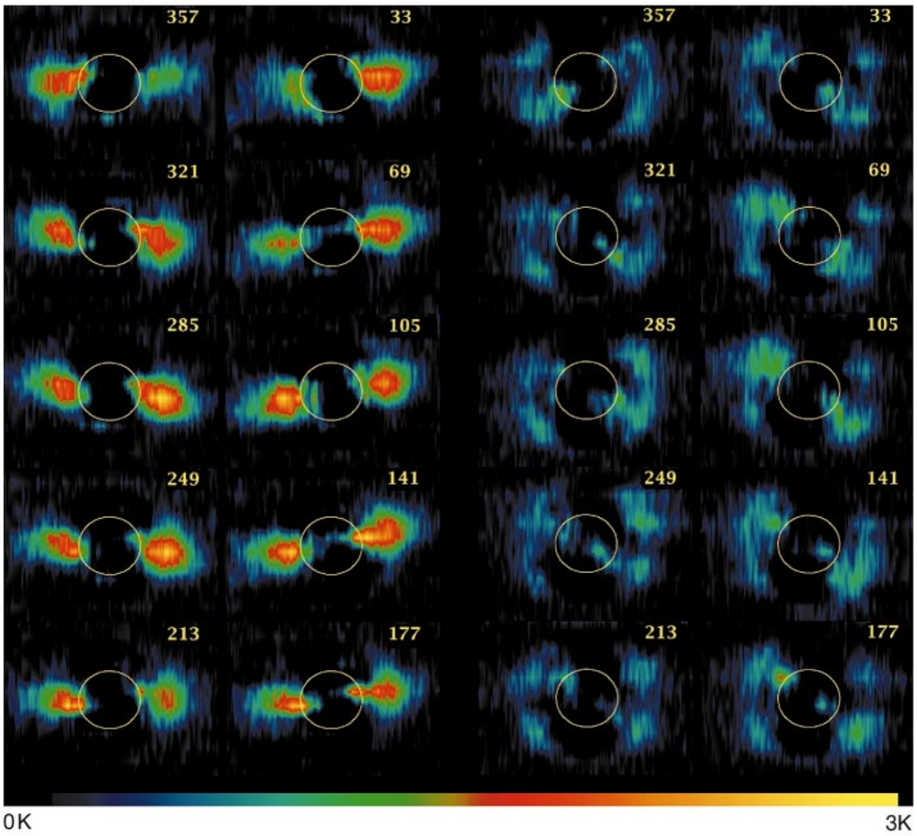

Figure 1 Colour maps of Jupiter's synchrotron emission taken by the Cassini spacecraft show the distribution of the ultra-relativistic electrons in Jupiter's inner radiation belts. Maps of horizontal linear polarization (left side) and vertical linear polarization (right side) show bright regions near 1.4 Jupiter radii (R_J), corresponding to peak emission by electrons of energy 50 MeV. The observation was carried out shortly after the closest approach to Jupiter, at a distance of $149R_J$ (~10^7 km) and a phase angle of approximately 75 degrees, using the 4-m on-axis Cassegrain reflector antenna that also serves as the Cassini primary communication antenna. The sub-spacecraft latitude on Jupiter was approximately 1.2 degrees south during the observation. The angular diameter of Jupiter was approximately 0.75 degrees. The colour scale is linear from 0 to 3 kelvin, black to yellow, as shown in the colour bar. Negative values (caused by noise and atmospheric model subtraction) have been set to zero. The 20-h observation was split into two sets of repeating raster scans, obtaining one complete rotation of Jupiter at each of two orthogonal polarizations. Each scan covered approximately $8R_J$ and $6R_J$ in east–west and north–south extent, respectively. A single scan, composed of 12 rasters separated by 0.18 degrees or approximately half-beam width (0.23 Jupiter angular diameters), required one hour to complete. Owing to the orientation of the magnetic field, emission originating near the magnetic equator is predominantly linearly polarized in the horizontal sense, while emission originating at higher latitudes is linearly polarized in the vertical sense. To remove thermal emission, a radiative transfer calculation for a nominal model of Jupiter's atmosphere was used to determine the brightness distribution across Jupiter's disk. The antenna beam pattern was determined from a composite of raster scans of the Sun and Jupiter (using an identical technique) obtained before the fly-by. The antenna gain and pointing varied less than 1% and 0.02 mrad, respectively, over the entire 20-h period of the observations. The relative distributions and amplitudes of the residuals as a function of polarization agree well with our model predictions. The variation between maps is related to the beaming curve, and has been studied extensively at 13-cm wavelength by Klein *et al.*[22]. The variation seen in the different panels shows that a form of beaming is present at 2.2 cm.

(DSN) operating at 2.2, 3.5 and 13 cm wavelengths (2.2 and 3.5 cm were used for thermal emission calibration only).

The narrow beaming of the synchrotron emission couples with the non-symmetrical magnetic field and the electron pitch angle distribution to produce variations as Jupiter rotates (the beaming curve). These variations can be seen in the Cassini polarization maps shown in Fig. 1. Cassini unambiguously detected synchrotron emission at a level of 0.44 ± 0.15 Jy (jansky; total integrated flux density adjusted to 4.04 AU). The synchrotron emission was observed to be approximately 1% of the measured thermal emission from Jupiter's disk. The level of synchrotron emission measured was less than estimated from simulations using the energy spectrum and the spatial distribution from current models[5,6]. The results demonstrate the existence of ultra-relativistic electrons near Jupiter and extend the measured nonthermal radio spectrum, providing a new constraint for models of Jupiter's radiation belts.

Observations with the VLA were carried out on 3 January 2001 when Earth was at a jovian declination of ~3 degrees. Figure 2 shows the VLA maps at 20 and 90 cm as a function of central meridian longitude. The total synchrotron emission measured was 5.15 ± 0.7 Jy at 90 cm (with this configuration the VLA cannot accurately measure the total flux at 20 cm). All four Stokes parameters were measured, although here we present only the images of total intensity, converted to brightness temperature. Observations from the DSN antennas in collaboration with the Goldstone–Apple Valley radio telescope (GAVRT) were obtained from November 2000 to March 2001. The GAVRT project also provided an opportunity for students to work with Cassini scientists, conducting ground-based observations and data analysis. Results from the DSN–GAVRT programme are shown in Fig. 3. The interpolated value of the synchrotron flux density on 3 January was 4.02 ± 0.08 Jy. Short-term variations at the 10% level are evident in the data set.

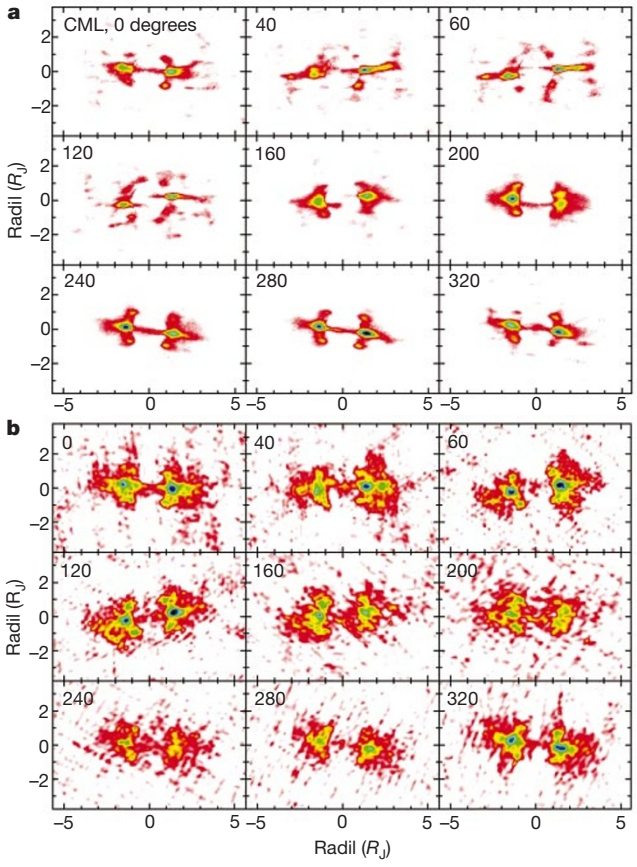

Figure 2 Colour maps of Jupiter's synchrotron radiation taken with the VLA show the distribution of less energetic relativistic electrons (as compared with Fig. 1). The brightest regions near $1.4R_J$ correspond to peak emission from electrons of energy 15 MeV (**a**, 20 cm), and 7 MeV (**b**, 90 cm). The observations were made for one full jovian rotation using the VLA operating in A configuration (36 km extent) with a synthesized beam width resolution of approximately 6 arcsec at 90 cm, and 1 arcsec at 20 cm (half-power beamwidth, HPBW). Two-dimensional images were constructed every 40 degrees of central meridian longitude (CML) from data recorded at the given CML ± 40 degrees. This is a standard construction technique, and thus images from different epochs can be compared directly. After calibration, Jupiter's thermal emission was subtracted (corresponding to a blackbody disk at 350 K), and background confusion sources were removed. For comparison purposes, the VLA data were adjusted to a standard distance of 4.04 AU.

The new synchrotron emission radio spectrum data is shown in Fig. 4. Data from an earlier epoch at one additional wavelength[8] is shown for completeness. At a frequency of 13.8 GHz (2.2 cm), the region of peak radio emission seen in the maps of Fig. 1 correspond to an average electron energy of ~50 MeV gyrating in a background magnetic field of approximately ~1.2 G (gauss). The VLA maps at 1.4 GHz and 333 MHz show regions of peak emission corresponding to average electron energies of ~15 MeV and ~7 MeV, respectively, in a ~1.2-G magnetic field. Because synchrotron radiation is emitted as a continuum, a wide range of electron energies contribute to the maps at each frequency and detailed modelling is required to estimate accurately the electron energy spectrum from the full set of multi-frequency observations. Figure 1 shows significant emission at radial distances $>2\,R_J$, suggesting much higher energy electrons (~100 MeV) at the larger radial distances. At a subset of central meridian longitudes, a double radiation belt is possibly indicated with the outer belt located just outside of Jupiter's main ring near $\sim 1.8\,R_J$, indicative of electron absorption by ring material.

The softer energy spectrum implied by the Cassini high-frequency observations indicates fewer ultra-relativistic electrons (~50 MeV) than predicted by current radiation-belt models. Current models of Jupiter's radiation belts use electron energy spectra based on *in situ* data from spacecraft (Pioneer[3] and Galileo probe[4]) and ground-based synchrotron observations. Although the *in situ* measurements suggested the existence of electrons greater than 20 MeV, the measurements lacked sufficient energy resolution to constrain the energy spectrum at high energies. Simulations of synchrotron emission using the Cassini-derived softer energy spectrum failed to match the intensity level of the lower range of frequencies observed. The preliminary modelling analysis suggests that both a softer energy spectrum and an increase in the number of electrons below 20 MeV are required to match the synchrotron emission spectrum in Fig. 4. The results suggest that the models of Jupiter's radiation belts[5] will probably require more modifications than were previously recommended[9] to estimate accurately the hazards to spacecraft venturing close to Jupiter.

The results reported here have direct effects on our understanding of Jupiter's radiation belts. The detection of synchrotron emission at 13.8 GHz implies that a steady source of ~50 MeV electrons must exist. This challenges current theories that have difficulty identifying a source even for the ~20-MeV electrons that are known to exist from previous observations. Secondly, the DSN–GAVRT 13-cm result confirms that the synchrotron emission can vary on relatively short timescales (days), which implies the existence of a process that can rapidly affect the distribution or number of ~20-MeV electrons trapped in Jupiter's strong magnetic field.

The most widely accepted theory postulates that the relativistic electrons originate in the solar wind or in the outer jovian magnetosphere and diffuse inward, gaining energy through conservation of the first and second adiabatic invariants[10–12]. This can account for ~10-MeV electrons near the peak of the synchrotron zone. However, additional acceleration mechanisms are required to explain higher energies. Efforts to model radial diffusion at Jupiter have failed to reproduce accurately a synchrotron emission radio

spectrum[12]. Additional sources of electron energization that are known to occur in the Earth's magnetosphere include local stochastic acceleration by wave–particle interactions[13,14], and acceleration by field-aligned potentials in the auroral zone[15]. Intense wave activity may also be responsible for rapid time variations in synchrotron emission[16]. Alternative mechanisms, which combine radial diffusive transport with wave–particle interactions, such as recycling and magnetic pumping[17–20], have also been proposed. Interaction between a very fast interplanetary shock and the Earth's magnetosphere has been proposed as a source of drift resonance

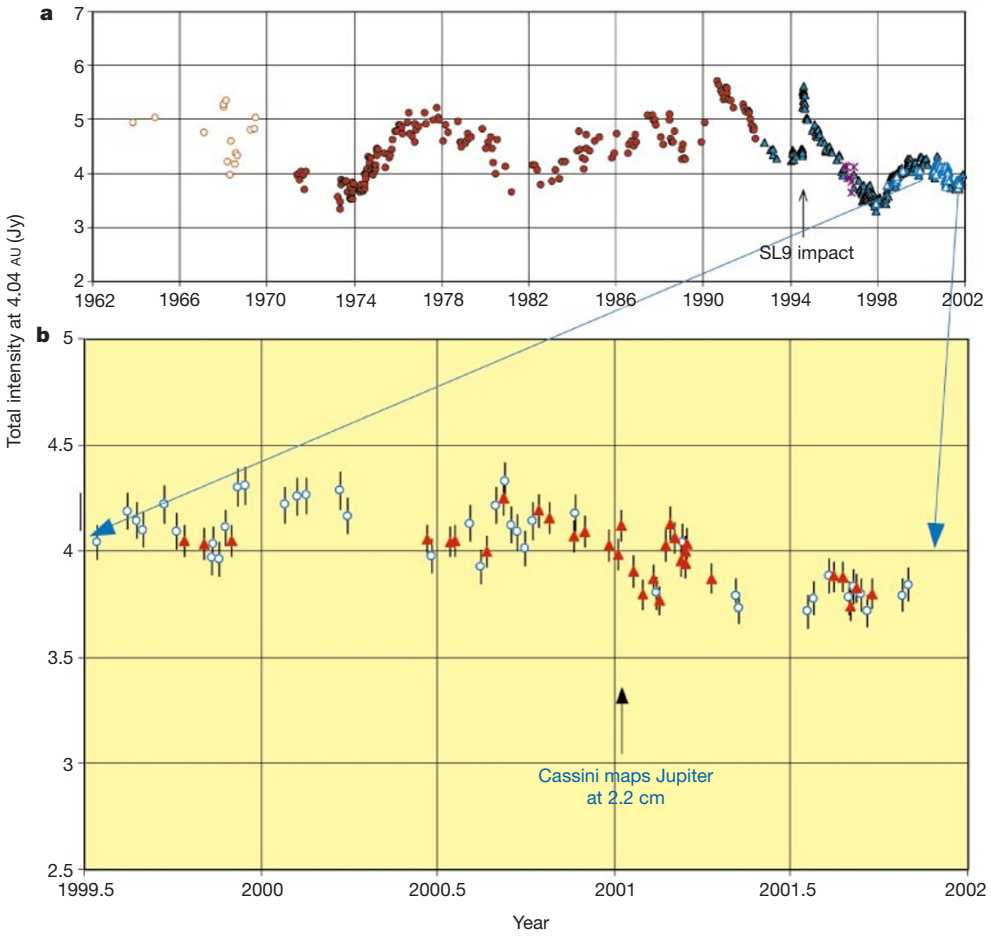

Figure 3 Variability of Jupiter's synchrotron radio emission shows evidence of long- and short-term variability. **a**, The history of long-term variations in the flux density of Jupiter's synchrotron radio emission at 13-cm wavelength. **b**, An expanded segment of the data taken over the past 2.5 yr that includes the Cassini fly-by period. Thermal flux density from the planet's atmosphere was subtracted from each measurement (assuming a disk temperature of 300 K) and results were normalized to a standard distance of 4.04 AU from Earth. Approximately 2,300 students and their teachers from 26 schools across the United States were part of the ground-based research team working through the GAVRT educational programme. The GAVRT data were merged with the ongoing NASA/JPL Jupiter Patrol to improve the time resolution of the data (JPL, Jet Propulsion Laboratory). The open circles are NASA/JPL Jupiter Patrol observations made with DSN antennas with apertures of 70 m and 34 m. GAVRT team observations made with 34-m-diameter antennas are represented by filled triangles. The agreement between the two data sets is approximately 1%. These events of 'modest' brightening appear to be intrinsic to Jupiter and are not caused by systematic errors in calibration or by discrete background radio sources that Jupiter passes in front of during its 12-yr orbital path along the ecliptic. Previous observations have suggested the presence of short-term variations in Jupiter's synchrotron radio emission[23–25]. SL9 indicates comet Shoemaker–Levy 9.

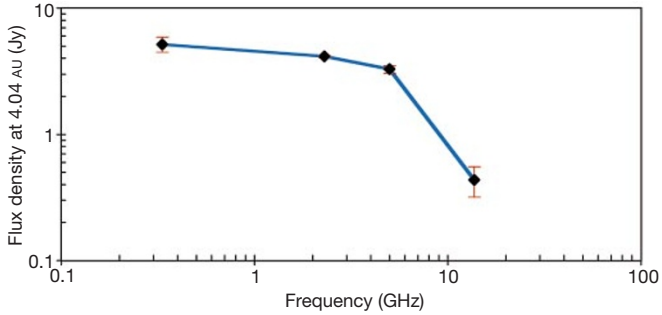

Figure 4 Jupiter's nonthermal radio spectrum indicates a softer than expected electron energy spectrum at high electron energies. The observed flux density of Jupiter's synchrotron emission observed with Cassini (13.8 GHz) is plotted alongside simultaneous measurements obtained using the DSN (2.3 GHz) and the VLA (0.333 GHz). Previous measurements at 6 cm (5 GHz) are shown for completeness[8]. All measurements are from January 2001 except for the 6-cm data from 1994. Error bars on the data are indicative of the preliminary nature of the results. Further analysis, including a recent Cassini beam calibration, is expected significantly to reduce the error bars on the data. The ratio between the integrated nonthermal flux densities measured at 2.2 cm and 13 cm is $S_{2.2}/S_{13} = 0.105 \pm 0.035$.

acceleration to explain the sudden appearance of relativistic electrons in the terrestrial 'Van Allen' radiation belts[21]. A similar process could exist at Jupiter, although analogies between the terrestrial and jovian magnetosphere are not always appropriate.

Thus, the inner radiation belts of Jupiter and Earth both contain extremely high-energy electrons that require substantial acceleration by processes other than adiabatic radial diffusion. These two magnetospheres are arguably the most explored examples of planetary magnetospheres in the Solar System and in many ways represent the archetype for magnetospheric physics. The fact that both magnetospheres contain electrons that require acceleration processes beyond radial diffusion suggests that this may be a fundamental property of all magnetospheres. This implies that our theoretical understanding of the global properties of magnetospheres may need revision and that the importance of local acceleration mechanisms may currently be underestimated. □

Received 18 September 2001; accepted 17 January 2002.

1. Burke, B. F. & Franklin, K. L. Observations of a variable radio source associated with the planet Jupiter. *J. Geophys. Res.* **60,** 213–215 (1955).
2. Berge, G. L. & Gulkis, S. in *Jupiter* (ed. Gehrels, T.) 621–692 (Univ. Arizona Press, Tucson, 1976).
3. Van Allen, J. A., Baker, D. N., Randall, B. A. & Sentman, D. D. Pioneer 11 observations of energetic particles in the Jovian magnetosphere. *Science* **188,** 459–462 (1975).
4. Fischer, H. M., Pehlke, E., Wibberenz, G., Lanzerotti, L. J. & Mihalov, J. D. High-energy charged particles in the inner Jovian magnetosphere. *Science* **272,** 856–858 (1996).
5. Divine, N. & Garrett, H. B. Charged particle distribution in Jupiter's magnetosphere. *J. Geophys. Res.* **88,** 6889–6903 (1983).
6. Levin, S. M. *et al.* Modeling Jupiter's synchrotron radiation. *Geophys. Res. Lett.* **28,** 903–906 (2001).
7. Elachi, C. *et al.* RADAR: The Cassini Titan radar mapper. *Space Sci. Rev.* (in the press).
8. Bird, M. K., Funke, O., Neidhofer, J. & De Pater, I. Multi-frequency radio observations of Jupiter at Effelsberg during the SL9 impact. *Icarus* **121,** 450–456 (1996).
9. Bolton, S. J. *et al.* Divine-Garrett model and Jovian synchrotron emission. *Geophys. Res. Lett.* **28,** 907–910 (2001).
10. Coroniti, F. V. in *The Magnetospheres of Earth and Jupiter* (ed. Formisano, V.) 391–410 (Reidel, Dordrecht, 1975).
11. Bolton, S. J., Gulkis, S., Klein, M. J., de Pater, I. & Thompson, T. J. Correlation studies between solar wind parameters and the decimetric radio emission from Jupiter. *J. Geophys. Res.* **94,** 121–128 (1989).
12. de Pater, I. & Goertz, C. K. Radial diffusion models of energetic electrons and Jupiter's synchrotron radiation 1. Steady state solution. *J. Geophys. Res.* **95,** 39–50 (1990).
13. Summers, D., Thorne, R. & Xiao, F. Relativistic theory of wave-particle resonant diffusion with application to electron acceleration in the magnetosphere. *J. Geophys. Res.* **103,** 20487–20500 (1998).
14. Summers, D., Thorne, R. M. & Xiao, F. Gyroresonant acceleration of electrons in the magnetosphere by superluminous electromagnetic waves. *J. Geophys. Res.* **106,** 10853–10868 (2001).
15. Carlson, C. W. *et al.* FAST observations in the downward auroral current region, energetic upgoing electron beams, parallel potential drops, and ion heating. *Geophys. Res. Lett.* **25,** 2017–2021 (1998).
16. Bolton, S. J. & Thorne, R. M. Assessment of mechanisms for Jovian synchrotron variability associated with comet SL9. *Geophys. Res. Lett.* **22,** 13–16 (1995).
17. Fujimoto, M. & Nishida, A. Monte Carlo simulation of the energization of Jovian trapped electrons by recirculation. *J. Geophys. Res.* **95,** 3841–3854 (1990).
18. Nishida, A. Outward diffusion of energetic particles from the Jovian radiation belt. *Geophys. Res. Lett.* **81,** 1771–1773 (1976).
19. Sentman, D. D., Van Allen, J. A. & Goertz, C. K. Recirculation of energetic particles in Jupiter's magnetosphere. *Geophys. Res. Lett.* **2,** 465–468 (1975).
20. Goertz, C. K. Energization of charged particles in Jupiter's outer magnetosphere. *J. Geophys. Res.* **83,** 3145–3150 (1978).
21. Li, X. *et al.* Simulation of the prompt energization and transport of radiation belt particles during the March 24, 1991, SSC. *Geophys. Res. Lett.* **20,** 2423–2426 (1993).
22. Klein, M. J., Thompson, T. J. & Bolton, S. J. in *Time Variable Phenomena in the Jovian System* (ed. Belton, M. J. S.) 151–155 (NASA Spec. Publ. 494, Lowell observatory, 1989).
23. Klein, M. J., Gulkis, S. & Bolton, S. J. in *Planetary Radio Emissions IV* (eds Rucker, H. O., Bauer, S. J. & Lecacheux, A.) 217–224 (Austrian Academy of Sciences Press, Vienna, 1996).
24. Galopeau, P. H. M., Gerard, E. & Lecacheux, A. Modifications of the synchrotron radiation belts of Jupiter: evidence for natural variations in addition to SL9 effects. *Planet. Space Sci.* **45,** 1197–1202 (1997).
25. Miyoshi, Y. *et al.* Observation of short-term variation of Jupiter's synchrotron radiation. *Geophys. Res. Lett.* **26,** 9–13 (1999).

Acknowledgements

We thank the Cassini Radar team, the Cassini Operations team, C. Hansen and J. Gross. The research reported in this paper was performed at the Jet Propulsion Laboratory, California Institute of Technology, under contract with the National Aeronautics and Space Administration.

Correspondence and requests for materials should be addressed to S.B. (e-mail: scott.j.bolton@jpl.nasa.gov).

The dusk flank of Jupiter's magnetosphere

W. S. Kurth*, D. A. Gurnett*, G. B. Hospodarsky*, W. M. Farrell†, A. Roux‡, M. K. Dougherty§, S. P. Joy‖, M. G. Kivelson‖, R. J. Walker‖, F. J. Crary¶ & C. J. Alexander#

** Department of Physics and Astronomy, University of Iowa, Iowa City, Iowa 52242, USA*
† NASA/Goddard Space Flight Center, Greenbelt, Maryland 20771, USA
‡ Centre d'étude des Environnements, Terrestre et Planétaires, Université de Versailles Saint-Quentin-en-Yvelines (CETP/UVSQ), 10–12 Avenue de l'Europe, F-78140 Velizy, France
§ Blackett Laboratory, Imperial College of Science and Technology, London SW7 2BZ, UK
‖ Institute of Geophysics and Planetary Physics, University of California, Los Angeles, California 90024, USA
¶ Space Physics Research Laboratory, University of Michigan, Ann Arbor, Michigan 48109, USA
 # Jet Propulsion Laboratory, 4800 Oak Grove Drive, Pasadena, California 91109, USA

Limited single-spacecraft observations of Jupiter's magnetopause have been used to infer that the boundary moves inward or outward in response to variations in the dynamic pressure of the solar wind[1–8]. At Earth, multiple-spacecraft observations have been implemented to understand the physics of how this motion occurs, because they can provide a snapshot of a transient event in progress. Here we present a set of nearly simultaneous two-point measurements of the jovian magnetopause at a time when the jovian magnetopause was in a state of transition from a relatively larger to a relatively smaller size in response to an increase in solar-wind pressure. The response of Jupiter's magnetopause is very similar to that of the Earth, confirming that the understanding built on studies of the Earth's magnetosphere is valid. The data also reveal evidence for a well-developed boundary layer just inside the magnetopause.

The measurements shown here are primarily from the radio and plasma wave science instruments on Cassini[9] and Galileo[10]; they make use of Cassini's fly-by of Jupiter centred on 30 December 2000 coupled with the extended Galileo orbital mission. Figure 1 shows the trajectories of Cassini and Galileo near Jupiter during the time interval surrounding the Cassini closest approach. Cassini first encountered the jovian bow shock at about 0419 spacecraft event time (SCET; HHMM UT at the spacecraft) on 28 December (day 363) 2000. As shown in Fig. 2, the shock is identified in the plasma wave data as a broadband burst of noise extending to about 1.5 kHz. The shock was preceded by about 3 h of Langmuir wave activity[11] at the electron plasma frequency f_{pe} near 2 kHz, giving an upstream solar-wind electron density n_e of 0.05 cm^{-3} using $n_e = (f_{pe}/8{,}980)^2$, where f_{pe} is measured in Hz. For several hours preceding the Langmuir wave activity, lower frequency, broadband, ion acoustic wave activity[12] in bursts was observed. We note that the Langmuir waves and ion acoustic waves are mutually exclusive. This would be consistent with Cassini's traversal of the ion foreshock into the electron foreshock. Cassini encountered the bow shock numerous times between 28 December 2000 and the end of the plotted interval. The bow shock was detected as late as early March 2001 to a distance of approximately 800 jovian radii (R_J).

On 9 January 2001 between 1250 and 2115 SCET, and again on 10 January between 0655 and 2035 SCET the Cassini radio and plasma wave instrument observed trapped continuum radiation[13,14], which is a clear indication that the spacecraft was within the jovian magnetosphere. Data from the Cassini plasma and magnetometer instruments confirmed the timing of the magnetopause crossings. A